Journal of Statistical Physics, Vol. 64, Nos. 5/6, 1991

Characteristics and Mechanisms of Electrorheological Fluids

Hans Conrad[1] **and Arnold F. Sprecher**[1]

Electrorheological (ER) fluids consist of suspensions of fine polarizable particles in a dielectric medium, which upon application of an electric field take on the characteristics of a solid in times of the order of milliseconds and reversibly return to liquid behavior upon removal of the field. The rheology, electrical characteristics, and structure of typical ER fluids are here reviewed. The proposed mechanisms and their accord with experimental data are discussed. Some directions for future research are mentioned.

KEY WORDS: Electrorheology; yield stress; Bingham solid; viscoelasticity; dielectric constant; electric field; fibrous structure; dipole moment; suspension; attractive force; viscosity; Mason number.

1. INTRODUCTION

Electrorheological (ER) fluids consist of suspensions of fine polarizable particles in a dielectric liquid, which upon application of an electric field take on the characteristics of a solid. This occurs reversibly, and in times of the order of milliseconds, and in general with low power requirements. Some examples of suspensions which exhibit ER behavior include corn starch in corn oil, silica gel in mineral oil, cellulose in transformer oil, and zeolite in silicone oil. Water adsorbed on or within the particles is important to the ER response of these systems; however, ER behavior has also been observed in systems which are essentially anhydrous, e.g., lithium polymethacrylate in chlorinated hydrocarbon oil and polymer-coated metal particles in silicone oil.

[1] Materials Science and Engineering Department, North Carolina State University, Raleigh, North Carolina 27695-7907.

822/64/5-6-12

The ER phenomenon was discovered by Winslow around the mid-1940s[1,2] and is often termed the Winslow effect. Earlier reviews of the ER effect are given in refs. 3–8. The objective of this paper is to review the current state of our knowledge regarding this interesting phenomenon. We will draw upon data in the literature by others as well as our own work.

2. RHEOLOGICAL CHARACTERISTICS

2.1. Experimental Apparatus and Terminology

Three types of equipment are generally employed in the laboratory to measure the rheological properties of an ER fluid: (a) a lateral shearing device attached to a conventional mechanical testing machine,[9–12] (b) a Couette cell,[13,14] and (c) parallel plate shear.[15] The lateral shearing device is generally employed for measurements at small shear strains and shear rates and the other two at high shear strains and rates. However, either type of equipment can be modified to cover a wider range of strains and rates.

An example of data obtained using the lateral shear device is shown in Fig. 1, that using a Couette cell in Fig. 2. The former is a plot of the

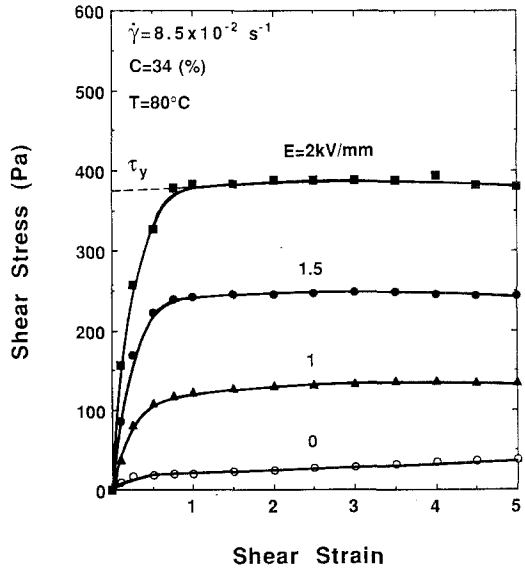

Fig. 1. Shear stress vs. shear strain curves for an ER fluid consisting of 34 wt % zeolite particles in silicone oil as a function of electric field E at 80°C and a shear rate of 8.5×10^{-2} sec^{-1}. A method used to define the static yield stress τ_y is shown. From Conrad *et al.*[12]

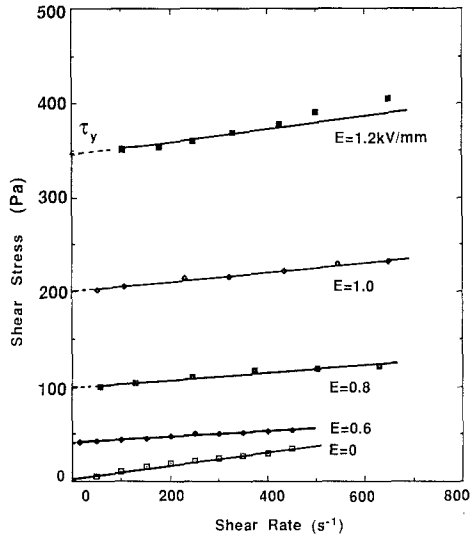

Fig. 2. Shear stress vs. shear rate as a function of electric field at 30°C for an ER fluid consisting of 8.9 wt % cellulose (10 wt % H_2O) in transformer oil. The common method for obtaining the dynamic yield stress is shown. From Uejima.[14]

shear stress τ vs. shear strain γ as might be determined for a structural material, the latter a plot of the shear stress τ vs shear rate $\dot{\gamma}$ as might be determined for a liquid. In some cases the transition from behavior at low shear strains to the steady-state type of behavior at large strains is not as smooth as shown in Fig. 1, but exhibits a "yield point" in which the stress first goes through a maximum and then decreases before reaching the steady-state condition,[9,12] the extrapolation of which is one definition of the static yield stress τ_y shown. Likewise, in Couette flow tests, the beginning of shear flow (the dynamic yield stress) may not be as well-defined as in Fig. 2, but may approach the steady state gradually or through a yield-point-type behavior. The shear stress τ vs. shear rate $\dot{\gamma}$ behavior illustrated in Fig. 2 approximates that of a Bingham solid:

$$\tau = \tau_y(E) + \eta_s \dot{\gamma} \tag{1}$$

where η_s is the viscosity of the suspension without an electric field E.

For purposes of comparison and for significance of the data, *it is important in both the lateral shear and Couette types of tests to define the yield stress (flow stress) as the shear stress at a given shear strain, strain rate, and temperature*, as is done for structural materials. In this context, the yield stress τ_y (static) as defined in Fig. 1 approximately equals the yield stress τ_y (dynamic) as defined in Fig. 2.

2.2. Effects of Electric Field Magnitude and Frequency, Composition, and Temperature on τ_y

2.2.1. Electric Field. The effect of electric field strength E on τ_y generally fits an equation of the form

$$\tau_y = AE^n \tag{2}$$

where A and n may be fluid and field dependent. n typically has values between 1 and 2.5, depending on the magnitude or range of field strengths considered. A similar effect of E on τ_y occurs for the dynamic yield stress. The most common value of n for a wide range of field strengths is 2[1,4,13–19]; $n = 1$ often occurs at relatively high values of E,[3,9,19] and $n > 2$ at low values.

In general, the yield stress of hydrous ER fluids (particles contain adsorbed water) remains relatively constant or shows only a modest decrease as the frequency f of the electric field is increased from DC to about 10^3 Hz; thereafter τ_y falls off rapidly. In one case an increase in τ_y with frequency initially occurred before passing through a maximum[22] (zeolite particles in a condenser oil). An increase in τ_y with f has been reported for anhydrous ER fluids containing polymer-coated metal particles.[23]

2.2.2. Composition. The strength of ER fluids generally increases with volume fraction ϕ of particles. However, beyond a certain concentration the effect may saturate or even decrease.[14] The initial increase in τ_y with ϕ is often of the form

$$\tau_y = B\phi^m \tag{3}$$

where B is a constant and $m = 2/3$ to $3/2$.[9,13,20]

It has been established that water adsorbed onto the particles is necessary for ER behavior in many fluids.[1,9,13,14,21] Similar to the effect of ϕ, an increase in the amount of adsorbed water first leads to an increase in strength, but then the effect generally saturates and ultimately may lead to a decrease in strength.[12,14]

2.2.3. Temperature. An example of the effect of temperature on the static yield stress of an ER fluid is presented in Fig. 3. The strength of the fluid initially increases as the temperature is raised, goes through a maximum, and then decreases with further increase in temperature. This type of behavior is characteristic of hydrous ER fluids.

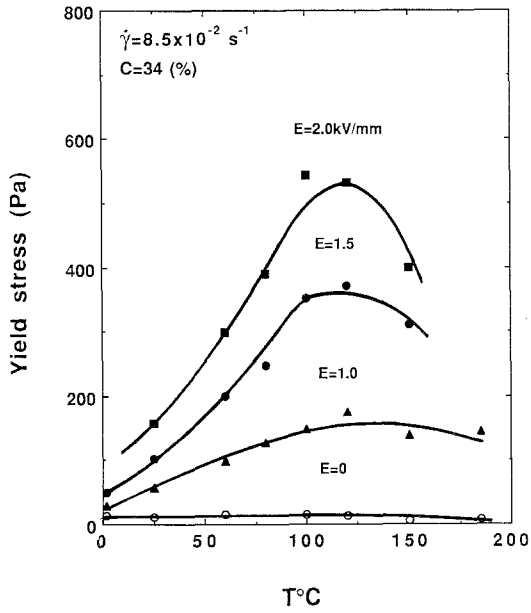

Fig. 3. Effect of temperature on the static yield stress τ_y as a function of electric field for 34 wt % zeolite particles in silicone oil. From Conrad *et al.*[12]

2.3. Viscoelastic Properties

Only limited data are available on the viscoelastic properties of ER fluids.[8,16,24] Jordon and Shaw[8] reported that the logarithm of the storage component of the shear modulus G' of a commercial fluid and a model fluid of polystyrene beads increased in a parabolic fashion with E up to 5 kV/mm, whereas Brooks *et al.*[16] found that the values of G (from torsional shear wave velocity) and of the storage modulus G' and loss modulus G'' (from attenuation of the shear waves) all passed through a sharp maximum as a function of E. The frequency of the shear wave in the latter work was 1200 rad/sec.

3. ELECTRICAL CHARACTERISTICS

A knowledge of the electrical characteristics of ER fluids is important from both scientific and technological viewpoints. From a scientific viewpoint they provide information needed to identify the operative mechanisms; from the technological side, they are important regarding power requirements and for control and switching.

3.1. Current Density

For the efficient operation of devices employing ER fluids it is desirable to have a current density j that is of the order of $\mu A/cm^2$. In static tests, j may remain relatively constant during straining[12] or decrease with strain.[11] Generally j increases more rapidly with E than Ohmic behavior (Fig. 4), giving

$$j = aE^b \tag{4}$$

where b has been found to have values between 1 and 5. Again, as in the case of τ_y, the value of the exponent b will depend on the ER system and the magnitude of E. For zeolite particles in silicone oil, j has been found to increase with temperature (up to 100°C) according to an Arrhenius-type behavior. For this ER fluid (zeolite particles in silicone oil), it was found that τ_y increased with j according to

$$\tau_y = A_j j^q \tag{5}$$

where $q = 1/5$.[12] On the other hand, Block and Kelley[25] reported that τ_y attained a maximum value at an intermediate electrical conductivity, the variation in conductivity being obtained by different poly(acene quinones) particles in chlorinated paraffin.

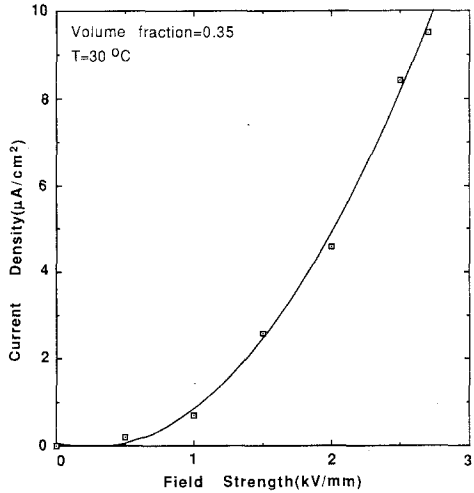

Fig. 4. Effect of electric field on the current density of an ER fluid consisting of lithium polymethacrylate in chlorinated hydrocarbon oil. From Brooks.[17]

3.2. Dielectric Constants

References pertaining to the frequency dependence of the permittivity of ER fluids are given in ref. 6. In general, at low shear rates the dielectric constant ε' decreases continuously with frequency f. However, with increase in shear rate a hump may occur in the curve of ε' vs. f, reflecting resonance.[25] For spherical particles, the frequency f_m at which resonance occurs was related to the shear rate $\dot{\gamma}$ by[25]

$$f_m = \dot{\gamma}/4\pi \tag{6}$$

Considering the dielectric loss constant ε'', this property generally passes through a maximum at some intermediate frequency, the value of which depends on the ER fluid system.[25]

The dielectric constant of an ER fluid has been found to be in reasonable accord with a linear rule of mixtures,[14,20,26] namely

$$\varepsilon_s = \varepsilon_p \phi + (1 - \phi)\, \varepsilon_f \tag{7}$$

where ε_p is the dielectric constant of the particles, ϕ their volume fraction, and ε_f the dielectric constant of the liquid phase. Further, both ε' and ε'' tend to increase with increase in temperature.[26]

4. ER FLUID STRUCTURE

Winslow[1] reported in his early work that upon application of an electric field the particles in an ER fluid align along the direction of the field in a chainlike or fibrous structure. He attributed the increased strength of the fluid to the force required to rupture the chains or fibers. Practically all known ER fluids exhibit this characteristic chainlike or fibrous structure. Optical microscopy[9,27] and the optical properties[15,28] have been employed to characterize the structure under both static (no shear) and dynamic (during shearing) conditions.

4.1. Static Structure

The development of the chainlike structure with increasing electric field in a model ER fluid of 27-μm glass beads in silicone oil is illustrated in Fig. 5. At small electric fields the particles begin to cluster, with a tendency to align along the field. This clustering increases with field until at $E = 0.5$ kV/mm complete chains first form across the gap between the electrodes. Further increase in E leads to an increase in the number of complete chains and less debris between the chains; also the thickness of the

chains increases. Figure 6 lists the stereological parameters pertaining to the model ER fluid structure which were measured. In the micrograph of Fig. 6a the meaning of some of the parameters is illustrated, namely $\lambda_c(\perp)$, the free spacing between chains; $X_c(\perp)$, the thickness of a chain; and $\lambda_c(\|)$, the free spacing of cross links. Figure 6b shows that the degree of alignment of the particles Ω_{12} increases rapidly with field to about 1 kV/mm and then levels off at higher fields, a slight decrease in the high-field value occurring with increase in area fraction A_A (volume fraction) of the glass beads. In

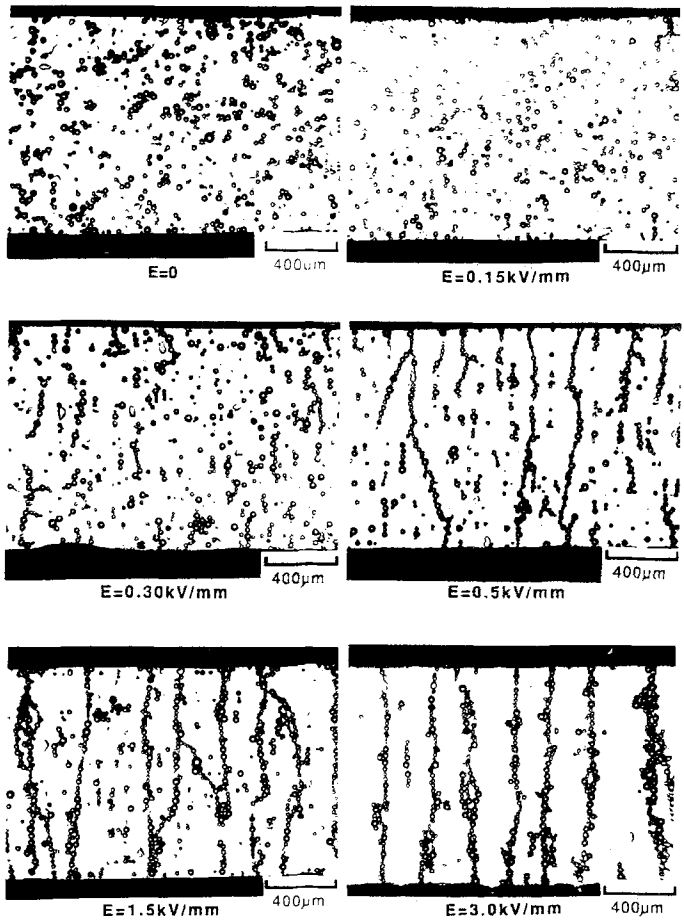

Fig. 5. Development of the chainlike structure in a model ER fluid (0.2 vol fraction of 27-μm glass beads in silicone oil) with increasing DC electric field: (a) $E=0$, (b) $E=0.15$ kV/mm, (c) $E=0.3$ kv/mm, (d) $E=0.5$ kV/mm, (e) $E=1.5$ kV/mm, and (f) E = 3 kV/mm. Electrodes are at the top and bottom of each photomicrograph. From Conrad *et al.*[27]

Fig. 6c it is seen that the remaining parameters which refer to the completed chains are relatively independent of E between 0.5 and 3 kV/mm, but depend sensitively on the volume fraction of beads. Since chain formation was only complete for $E \geqslant 0.5$ kV/mm, these parameters could only be determined for E greater than this critical value. Worthy of mention is that the main features of the structure developed in times faster than the eye

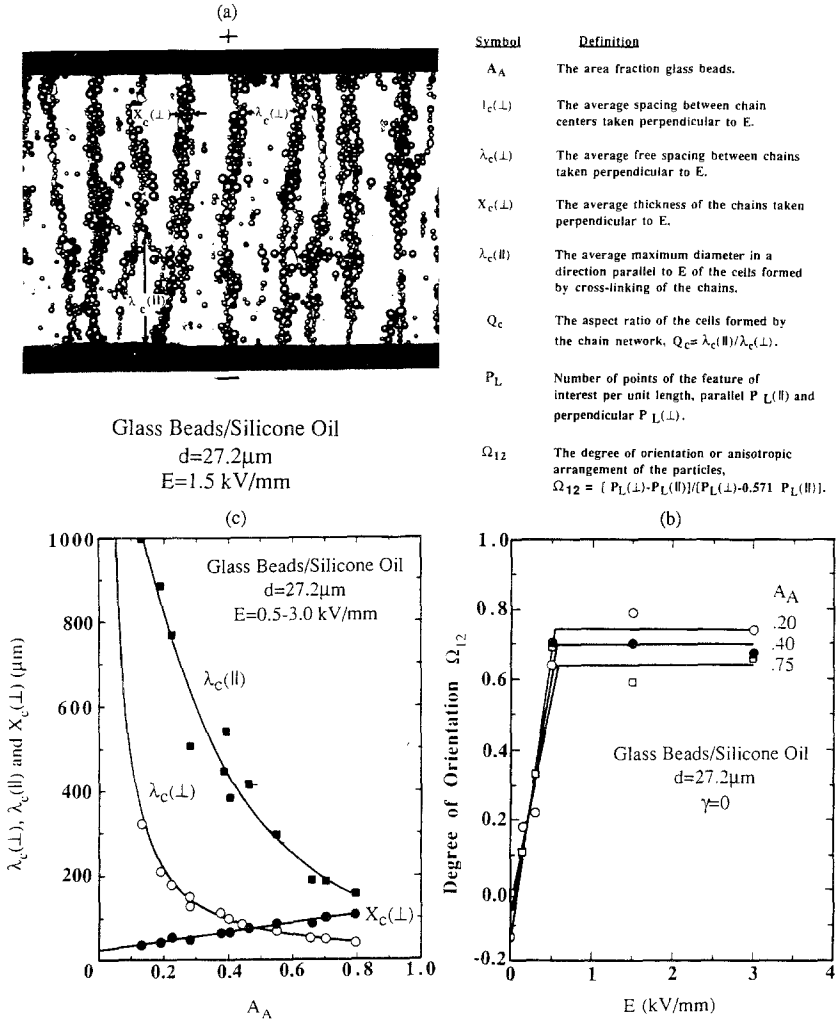

Fig. 6. Stereological parameters used to characterize the structure of the model ER fluid and the effects of electric field E and volume fraction of beads A_A on some of these parameters. Data from Conrad *et al.*[27]

could follow. However, adjustments and movements of isolated beads occurred for some time thereafter.

Smith and Fuller[28] studied the structure of suspensions of 49- and 130-nm silica spheres in cyclohexane by measurements of birefringence and dichroism as a function of time following application of the electric field and the magnitude of the field. The time to reach 50% of the steady-state value of birefringence or dichroism decreased with field from about 0.1 sec at $E = 1$ kV/mm to about 0.05 sec at 4 kV/mm. The steady-state values increased rapidly with field to about 1 kV/mm and then changed only little thereafter, similar to what was observed for the orientation parameter Ω_{12} for 27-μm glass beads in silicone oil (Fig. 6). Also similar to the behavior observed for the glass beads by optical microscopy, the degree of alignment of the fine silica particles determined by the optical property measurements decreased as the volume fraction of particles was increased.

4.2. Dynamic Structure

Only scant studies have been made of the structure of ER fluids during shearing. An example of the results obtained by the present authors is shown in Fig. 7. The left side of the bottom part of the figure gives the velocity profile, the right side the fluid structure. At the lower fields and shear rates ($\dot{\gamma} \leqslant 1\ \text{sec}^{-1}$), the chains continually ruptured and reformed, maintaining a homogeneous fiber structure across the electrode gap. With increase in field, a zone devoid of fibers developed in the middle of the gap and shearing mainly took place in this central region. An electrodynamic effect occasionally occurred, especially at high fields (1–2 kV/mm^2), destroying the fibrous structure, which, however, reformed if shearing was ceased. At higher shear rates ($\dot{\gamma} > 1\ \text{sec}^{-1}$) fluid motion was more turbulent and the formation of a zone without fibers was not well defined. Moreover, the turbulence frequently destroyed the fibrous structure completely.

5. MECHANISMS

5.1. Theory

Two basic phenomena have been proposed to explain the increase in shear strength of ER fluids, namely water bridging and polarization of the particles. In the bridging phenomena it is assumed that water molecules associated with mobile ions are within the pores of the particles. Upon application of an electric field the mobile ions move to one end of the particle, carrying the water with them, which then forms a bridge with an adjacent particle. The interfacial tension between the water and the ER

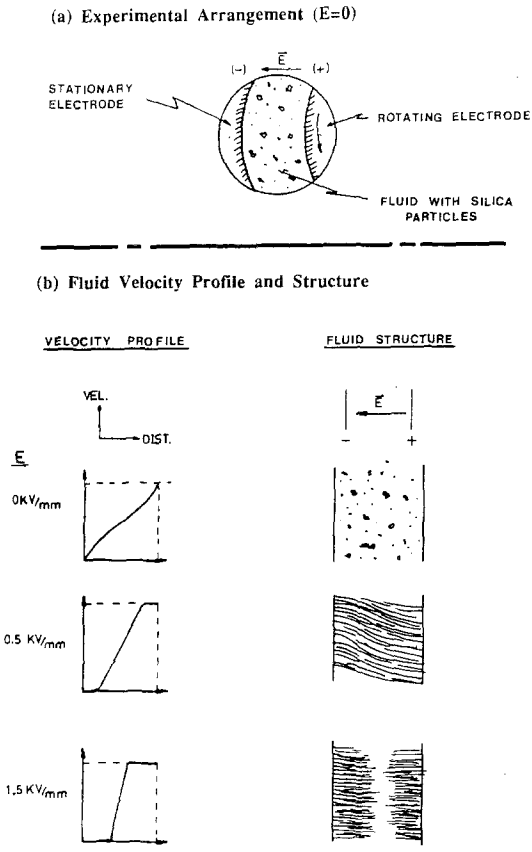

Fig. 7. Schematics of the structure of a model ER fluid (27-μm glass beads in silicone oil) under dynamic shearing. From Sprecher *et al.*[9]

carrier fluid then provides a source of shear resistance. Since the bridging mechanism is covered in some detail by Stangroom, we will restrict our discussion to mechanisms based on polarization.

The force between dipoles has been calculated rigourously for the case of two point dipoles in a uniform electric field separated by a distance R much greater than their radii a:

$$f_d = \left(\frac{6}{4\pi\varepsilon_f}\right)\frac{p^2}{R^4} \tag{8}$$

where p is the dipole moment and ε_f the total permittivity of the fluid. p is given by

$$p = 4\pi\varepsilon_0 a^3 E K_f \left[\frac{K_p - K_f}{K_p + 2K_f}\right] \tag{9}$$

where ε_0 is the permittivity of free space and $K = \varepsilon/\varepsilon_0$ is the total relative permittivity, the subscripts p and f referring to the particle and fluid, respectively. Combining Eqs. (8) and (9) and recognizing that $K = K' + iK''$, where $K'' = \sigma/\omega$ (σ = conductivity) and $\omega = 2\pi f$ (f = frequency), we obtain

$$f_d = \frac{24\pi a^6 \varepsilon_0 K_f (\beta E)^2}{R^4} \tag{10}$$

where

$$\beta = (K_p - K_f)/(K_p + 2K_f) \tag{11}$$

The value of f_d given by Eq. (10) is for particles aligned in the direction of the applied field. By considering the angle θ with respect to the field it is found that f_d is a maximum and attractive when $\theta = 0$, i.e., when the particles are aligned in the field, and repulsive when $\theta = 90°$, i.e., when the particles are aligned perpendicular to the field. The theory is thus in qualitative accord with the chainlike structure observed in ER fluids.

To quantitatively check the predictions of Eqs. (8)–(10), the present authors measured the force required to deform and rupture in shear a chain of particles consisting of 3–5 glass beads in silicone oil.[30] Figure 8 shows that the force to rupture the chain varied as E^2. However, the dipole

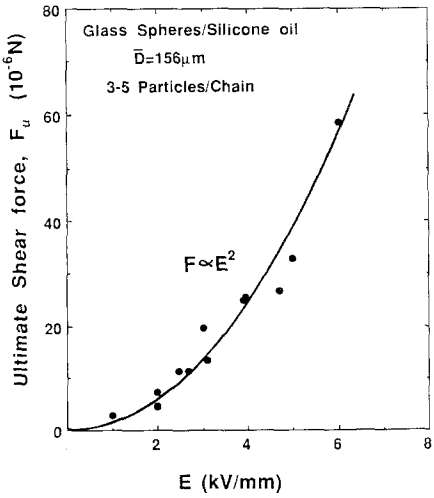

Fig. 8. Shear force required to rupture a chain of 3–5 particles (156-μm humidified glass beads) in silicone oil vs. the electric field. The solid line represents the shear force being proportional to E^2. From Sprecher *et al.*[29]

moment derived from these measurements was about an order of magnitude larger than predicted by Eq. (9); see Fig. 9. It was concluded that this discrepancy between the measured values of the dipole moment and the prediction of Eq. (9) resulted from the fact that the theory is based on two *widely-spaced* point dipoles in a uniform electric field, whereas the measurements are made on a chain of *nearly contacting* particles. The interaction force between particles aligned in a chain has been calculated employing an expansion of the potential which satisfies the Laplace equation.[30] The calculations predict the possibility of *an order of magnitude concentration* of the electric field near the particle contact region and in turn a two orders of magnitude higher interaction force than that given by Eq. (10). The following expression was obtained for the force of attraction F_d between *nearly contacting* spherical particles in a chain:

$$F_d = 0.9\alpha^2 f_d \tag{12}$$

where $\alpha = E_l/E$ is the ratio of the local field to the applied field between the electrodes and f_d is given by Eq. (10). The agreement of the measured force to rupture the chain of glass beads with the prediction of Eq. (12) compared to Eq. (10) is shown in Fig. 10.

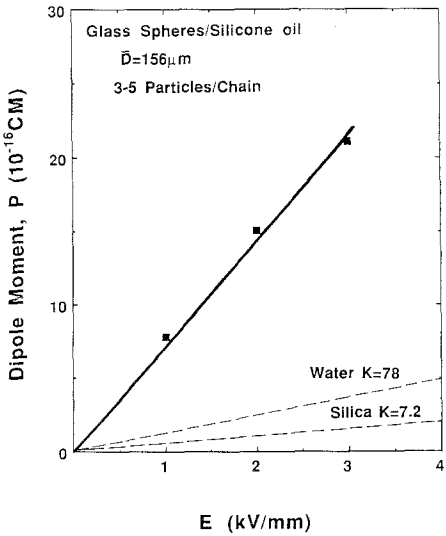

Fig. 9. Experimentally derived dipole moment vs. electric field for humidified glass beads. Also given are the values calculated for spheres consisting entirely of silica or of water. From Sprecher *et al.*[29]

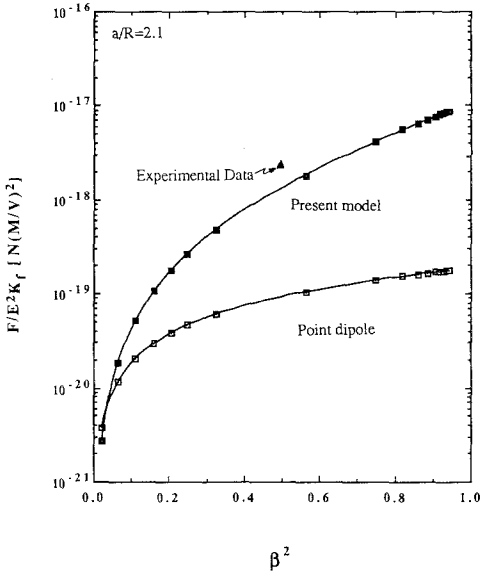

Fig. 10. Logarithm of the normalized particle–particle interaction force vs. β^2 for the following: point-dipole approximation, nearly contacting spheres in a chain, and measured force to rupture a chain of glass beads in silicone oil. Details regarding the calculations given in Chen *et al.*[30]

5.2. Application to Rheological Behavior

It is expected that the yield stress may be proportional to the force required to rupture the chain structure and therefore according to Eq. (10) that τ_y be proportional to E^2, which is frequently observed. Klingenberg and Zukoski[31] developed the following expression for the yield stress:

$$\tau_y = 18\phi F_{\max}\left\{1 - \frac{(\pi/6)^{1/2}}{(l/a)\tan\theta_{\max}\,\phi^{1/2}}\right\} \tag{13}$$

where $F_{\max}$ is the maximum restoring force, l is the electrode spacing, and $\theta_{\max}$ is the angle between the line of centers of the particles and the field at which rupture of the chains occurs. They obtained reasonable agreement between the data of Marshall *et al.*[20] and Eq. (13).

Employing Eq. (12) and assuming that the polarized particles are aligned in a chainlike structure and that each chain consists of a single row of contacting particles, the present authors obtained for the shear strength of an ER fluid[30,32]

$$\tau_y = \phi\varepsilon_0 K_f(\alpha E\beta)^2 \tag{14}$$

The agreement between the measured values of τ_y as a function of temperature for zeolite particles in silicone oil given in ref. 32 and those predicted by Eq. (14) is shown in Fig. 11.

Another approach employed to compared rheological behavior with theoretical predictions is to consider the apparent viscosity $\eta_a = \tau/\dot{\gamma}$. Starting with the observation that ER fluids approximates a Bingham solid, we obtain upon dividing both sides of Eq. (1) by $\dot{\gamma}$

$$\tau/\dot{\gamma} = \tau_y/\dot{\gamma} + \eta_s \tag{15}$$

Further, upon dividing both sides of Eq. (15) by η_s and taking $\tau_y = AF$ (where A is a constant) gives

$$\frac{\eta_a}{\eta_s} = \left(\frac{A24\pi a^6 \varepsilon_0 E^2 K_f \beta^2}{\dot{\gamma}\eta_s R^4}\right) + 1 \tag{16}$$

or, dividing by η_f,

$$\frac{\eta_a}{\eta_f} = \left(\frac{A24\pi a^6 \varepsilon_0 E^2 K_f \beta^2}{\dot{\gamma}\eta_f R^4}\right) + \frac{\eta_s}{\eta_f} \tag{17}$$

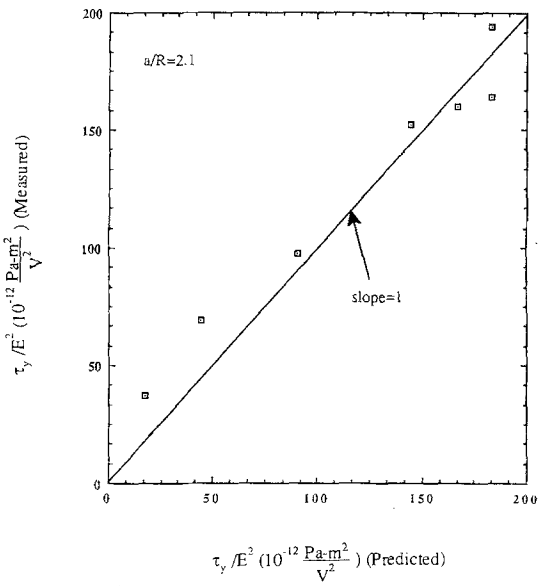

Fig. 11. Measured vs. predicted values of τ_y for zeolite particles in silicone oil. Data from Conrad *et al.*[32]

where η_f is the viscosity of the carrier fluid. Equations (16) and (17) reduce to

$$\eta_a/\eta_s = B/Mn + 1 \tag{16a}$$

or

$$\eta_a/\eta_f = B/Mn + \eta_s/\eta_f \tag{17a}$$

where $B = A\,24\pi a^6 K_f/2R^4$ and $Mn = \dot{\gamma}\eta_f/2\varepsilon_0 E^2\beta^2$, the so-called Mason number, which gives the ratio of the viscous flow force to the polarization force.[20] Since $\eta_s \approx \eta_f$, Eqs. (16a) and (17a) are essentially equivalent. Moreover, a log–log plot of η_a/η_f vs $\dot{\gamma}$ should yield a curve with initial slope -1 and approach a value of 1 at high shear rates, i.e., at large values of *Mn*. By this means Marshall *et al.*[20] were able to correlate the effects of $\dot{\gamma}$, E, T, and ϕ on the rheological behavior of an ER fluid consisting of lithium polymethocrylate particles in chlorinated hydrocarbon oil; see, for example, Fig. 12.

The concept of the Mason number has also been employed by Bonnecaze and Brady[33] in their computer simulation of the rheology of ER fluids. The simulation was applied to an unbounded monolayer of spherical dielectric particles in a Newtonian fluid subjected to simple shear flow with an orthogonal electric field. Reasonable agreement was obtained

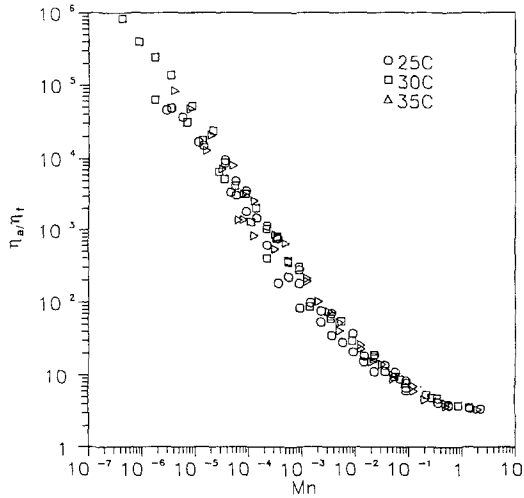

Fig. 12. Relative viscosity vs. Mason number for an ER fluid (0.23 vol fraction lithium polymethocrylate in chlorinated hydrocarbon oil) tested at 25, 30, and 35°C. From Marshall *et al.*[20]

between the simulated curve of the relative velocity vs. *Mn* as a function of electric field and the experimental data of Marshall *et al.*[20]

Turning to the shear modulus of ER fluids, only modest success has been achieved in deriving the storage and loss moduli from a consideration of polarization forces.[15,16]

Finally, very little is known regarding the detailed atomic mechanisms by which polarization of the particles is achieved and its time dependence. Of interest in this regard is the finding[12,32] that the activation energy for the effect of temperature on the current density and yield stress in ER fluids containing zeolite particles is the same as that for the diffusion of the Na^+ ions along the zeolite channels. This suggests that in this ER system the polarization and its rate dependence are governed by the mobility of the Na^+ ions.

6. CONCLUSIONS

a. Many of the characteristics of ER fluids have been identified.

b. There exists considerable evidence that polarization forces are responsible for the increased shear resistance of many ER fluids.

c. A refinement of the point dipole approximation which takes into account the alignment of particles by the electric field into a chainlike structure gives reasonable agreement with experimental measurements of the shear strength of ER fluids under quasistatic conditions.

d. Additional experimental investigations are needed to check the general validity of the derived theoretical equations for both static and dynamic shearing conditions. Also needed are studies to define the atomic mechanisms by which polarization occurs.

ACKNOWLEDGMENTS

The authors gratefully acknowledge support of their work on ER fluids by the National Science Foundation under NSF award CBT-8714515, the Ford Motor Company, and the NCSU University/Industry Consortium on ER Fluids.

REFERENCES

1. W. M. Winslow, U. S. Patent No. 2,417,850 (March 25, 1947); *J. Appl. Phys.* **20**:1137 (1949).
2. W. M. Winslow, in *Proceedings of the 2nd International Conference on Electrorheological Fluids*, J. D. Carlson, A. F. Sprecher, and H. Conrad, eds. (Technomic Publ. Co., Lancaster-Basel, 1990), p. 1X.

3. J. E. Stangroom, *Phys. Technol.* **14**:290 (1983).
4. C. F. Zukoski and J. W. Goodwin, in *IEEE IECON'86* (1986), p. 9.
5. H. Conrad and A. F. Sprecher, in *Proceedings Adv. Materials Conference*, J. G. Morse, ed. (TMS, 1987), p. 63.
6. H. Block and J. P. Kelley, *J. Phys. D: Appl. Phys.* **21**:1661 (1988).
7. A. P. Gast and C. F. Zukoski, *Adv. Colloid Interface Sci.* **30**:153 (1989).
8. T. C. Jordon and M. T. Shaw, *IEEE Trans. Electrical Insulation* **24**:849 (1989).
9. A. F. Sprecher, J. D. Carlson, and H. Conrad, *Mat. Sci. Eng.* **95**:187 (1987).
10. N. G. Stevens, J. L. Sproston, and R. Stanway, Trans. *ASME* **54**:456 (1987).
11. H. Conrad, A. R. Shamala, and A. F. Sprecher, in *Proceedings of the 1st International Symposium on Electrorheological Fluids*, H. Conrad, A. F. Sprecher and J. D. Carlson, eds. (NCSU Engr. Publ., Raleigh, North Carolina, 1989), p. 47.
12. H. Conrad, Y. Chen, and A. F. Sprecher, in *Proceedings of the 2nd International Conference on Electrorheological Fluids*, J. D. Carlson, A. F. Sprecher, and H. Conrad, eds., (Technomic Publ. Co., Lancaster-Basel, 1990), p. 252.
13. D. L. Klass and T. W. Martinek, *J. Appl. Phys.* **38**:67 (1967).
14. H. Uejima, *Jpn. J. Appl. Phys.* **11**:319 (1972).
15. T. C. Jordon and M. T. Shaw, in *Proceedings of the 2nd International Conference on Electrorheological Fluids*, J. D. Carlson, A. F. Sprecher, and H. Conrad, eds. (Technomic Publ. Co., Lancaster-Basel, 1990), p. 231.
16. D. Brooks, J. Goodwin, C. Hjelm, L. Marshall, and C. Zukoski, *Colloids Surf.* **18**:293 (1986).
17. D. A. Brooks, in *Proceedings of the 2nd International Conference on Electrorheological Fluids*, J. D. Carlson, A. F. Sprecher, and H. Conrad, eds. (Technomic Publ. Co., Lancaster-Basel, 1990), p. 37.
18. G. Opperman, G. Penners, M. Schulze, G. Marquardt, and R. Findt, in *Proceedings of the 2nd International Conference on Electrorheological Fluids*, J. D. Carlson, A. F. Sprecher, and H. Conrad, eds. (Technomic Publ. Co., Lancaster-Basel, 1990), p. 287.
19. D. A. Brooks, in *Proceedings of the 1st International Symposium on Electrorheological Fluids*, H. Conrad, A. F. Sprecher, and J. D. Carlson, eds. (NCSU Engr. Publ., Raleigh, North Carolina, 1989), pp. 63.
20. L. Marshall, J. W. Goodwin, and C. F. Zukoski, *J. Chem. Soc. Faraday Trans.* **85**:2185 (1989).
21. F. E. Filisko and L. H. Radzilowski, *J. Rheol.* **34**:539 (1990).
22. A. F. Sprecher, Y. Chen, and H. Conrad, unpublished research NCSU (1990).
23. A. Inoue, in *Proceedings of the 2nd International Conference on Electrorheological Fluids*, J. D. Carlson, A. F. Sprecher, and H. Conrad, eds. (Technomic Publ. Co., Lancaster-Basel, 1990), p. 176.
24. T. C. Jordon and M. T. Shaw, Paper No. 44B, Annual Meeting, American Institute of Chemical Engineers, December 1988.
25. H. Block and J. P. Kelley, in *Proceedings of the 1st International Symposium on Electrorheological Fluids*, H. Conrad, A. F. Sprecher, and J. D. Carlson, eds. (NCSU Engr. Publ. Raleigh, North Carolina, 1989), p. 1.
26. D. L. Klass and T. W. Martinek, *J. Appl. Phys.* **38**:75 (1967).
27. H. Conrad, M. Fisher, and A. F. Sprecher, in *Proceedings of the 2nd International Conference on Electrorheological Fluids* (Technomic Publ. Co., Lancaster-Basel, 1990), p. 63.
28. K. L. Smith and G. G. Fuller, in *Proceedings of the 1st International Symposium on Electrorheological Fluids*, H. Conrad, A. F. Sprecher, and J. D. Carlson eds. (NCSU Engr. Publ., Raleigh, North Carolina, 1989), p. 27.
29. A. F. Sprecher, Y. Chen, and H. Conrad, in *Proceedings of the 2nd International*

Conference on Electrorheological Fluids, J. D. Carlson, A. F. Sprecher, and H. Conrad, eds. (Technomic Publ. Co., Lancaster-Basel, 1990), p. 82.
30. Y. Chen, A. F. Sprecher, and H. Conrad, Particle–particle dipole interactions in electrorheological fluids, *J. Appl. Phys.*, to appear.
31. D. J. Klingenberg and C. F. Zukoski, *Langmuir* **6**:15 (1990).
32. H. Conrad, A. F. Sprecher, Y. Choi, and Y. Chen, The temperature dependence of the electrical properties and strength of electrorheological fluids, *J. Rheol.*, to appear.
33. R. T. Bonnecaze and J. F. Brady, in *Proceedings of the 2nd International Conference on Electrorheological Fluids*, J. D. Carlson, A. F. Sprecher, and H. Conrad, eds. (Technomic Publ. Co., Lancaster-Basel, 1990), p. 27.